Experimental Neurology xxx (xxxx) 114204

Contents lists available at ScienceDirect

Experimental Neurology

journal homepage: www.elsevier.com/locate/yexnr

Research paper

Environmental enrichment improves traumatic brain injury-induced behavioral phenotype and associated neurodegenerative process

Victor Tapias[a,b,c,*], Eleni H. Moschonas[d,e,f], Corina O. Bondi[d,e,f,g], Vincent J. Vozzella[d,e], Iya N. Cooper[d,e], Jeffrey P. Cheng[d,e], Naima Lajud[d,e,h], Anthony E. Kline[d,e,f,i,j,k,**]

[a] Department of Neurology, Pittsburgh Institute for Neurodegenerative Diseases, University of Pittsburgh, Pittsburgh, PA 15260, USA
[b] Excellence Unit of the Institute of Genetics and Molecular Biology (IBGM) – Consejo Superior de Investigaciones Científicas, Valladolid 47003, Spain
[c] Department of Biochemistry and Molecular Biology and Physiology, School of Medicine, University of Valladolid, Valladolid 47003, Spain
[d] Physical Medicine & Rehabilitation, University of Pittsburgh, Pittsburgh, PA, USA
[e] Safar Center for Resuscitation Research, University of Pittsburgh, Pittsburgh, PA, USA
[f] Center for Neuroscience, University of Pittsburgh, Pittsburgh, PA, USA
[g] Neurobiology, University of Pittsburgh, Pittsburgh, PA, USA
[h] División de Neurociencias, Centro de Investigación Biomédica de Michoacán - Instituto Mexicano del Seguro Social, Morelia, MX
[i] Center for the Neural Basis of Cognition, University of Pittsburgh, Pittsburgh, PA, USA
[j] Critical Care Medicine, University of Pittsburgh, Pittsburgh, PA, USA
[k] Psychology, University of Pittsburgh, Pittsburgh, PA, USA

ARTICLE INFO

Keywords:
Traumatic brain injury
Environmental enrichment
Behavior
Cognition
Oxidative stress
Inflammation

ABSTRACT

Traumatic brain injury (TBI) causes persistent cognitive impairment and neurodegeneration. Environmental enrichment (EE) refers to a housing condition that promotes sensory and social stimulation and improves cognition and motor performance but the underlying mechanisms responsible for such beneficial effects are not well defined. In this study, anesthetized adult rats received either a moderate-to-severe controlled cortical impact (CCI) or sham surgery and then were housed in either EE or standard conditions. The results showed a significant increase in protein nitration and oxidation of lipids, impaired cognition and motor performance, and augmented *N*-methyl-D-aspartate receptor subtype-1 (NMDAR1) levels. However, EE initiated 24 h after CCI resulted in reduced oxidative insult and microglial activation and significant improvement in beam-balance/walk performance and both spatial learning and memory. We hypothesize that following TBI there is an upstream activation of NMDAR that promotes oxidative insult and an inflammatory response, thereby resulting in impaired behavioral functioning but EE may exert a neuroprotective effect via sustained downregulation of NMDAR1.

1. Introduction

Traumatic brain injury (TBI), a penetrating or closed form of acquired brain injury, is a leading cause of persistent disabilities and death worldwide (Hyder et al., 2007). The deleterious effects of TBI are not confined to the salient motor, affective, and cognitive dysfunction that diminish life quality but are compounded by the negative impact on occupational and social functioning. TBI can be classified as mild, moderate, or severe, depending on whether the injury causes unconsciousness, how long unconsciousness lasts, and the severity of symptoms. TBI with loss of consciousness is associated with a 4–5-fold increased risk of dementia and neurodegenerative diseases, including Alzheimer's disease (AD), Parkinson's disease, and frontotemporal dementia (Crane et al., 2016; LoBue et al., 2016; Gardner et al., 2018). In addition, exposure to repeated mild TBI may increase the risk of developing chronic traumatic encephalopathy, a progressive tauopathy (McKee et al., 2013).

Compelling evidence has demonstrated that sustained oxidative stress plays a crucial role in the onset and pathogenesis of TBI. Modification of tyrosine residues in proteins by NO•-derived species leads to 3-nitrotyrosine (3-NT) formation. Evidence of protein nitration has been described in the mouse cerebral cortex, rat hippocampus, and CSF samples from TBI patients (Darwish et al., 2007; Deng et al., 2007; Readnower et al., 2010). Another important oxidative stress-induced-

* Correspondence to: V. Tapias, Institute of Genetics and Molecular Biology (IBGM) – CSIC, University of Valladolid, C. Sanz y Fores 3, 47003 Valladolid, Spain.
** Correspondence to: A.E. Kline, Physical Medicine & Rehabilitation, Critical Care Medicine, and Psychology, Safar Center for Resuscitation Research, University of Pittsburgh School of Medicine, Children's Hospital of Pittsburgh, John G. Rangos Research Center, Room 6126, 4401 Penn Avenue, Pittsburgh, PA 15224, USA.
E-mail addresses: victor.tapias@uva.es (V. Tapias), klineae@upmc.edu (A.E. Kline).

https://doi.org/10.1016/j.expneurol.2022.114204
Received 8 June 2022; Received in revised form 13 July 2022; Accepted 10 August 2022
0014-4886/

modification is lipid peroxidation (LPO). Malondialdehyde (MDA), the most mutagenic LPO-derived product can interact with proteins and DNA to form stable adducts, which leads to structural and functional alterations and subsequent strong immune responses and mitochondrial deficiencies (Jove et al., 2020). 4-hydroxynonenal (4-HNE) can interfere with mitochondrial respiration, DNA synthesis, and calcium (Ca^{2+}) homeostasis (Chandra and Srivastava, 1997). Acrolein is the most reactive product of LPO and is an initiator of oxidative stress by adducting nucleophilic groups found on lipids, proteins, and nucleic acid. Acrolein inhibits mitochondrial respiration at different levels although does not alter the enzymatic activities of the electron transport chain (Picklo and Montine, 2001). Isoprostanes (IsoP) are prostaglandin-like compounds generated from the free radical-catalyzed peroxidation of essential fatty acids (mainly arachidonic acid) and show a stable metabolic profile, which make them more suitable markers of LPO (Beal et al., 2020). Several studies have demonstrated a robust increase in the levels of LPO-derived metabolites, such as MDA and 4-HNE, in diverse experimental models of TBI (Solaroglu et al., 2005; Sharma et al., 2010).

A mechanical consequence of brain trauma involves disruption of the blood–brain barrier (BBB), which leads to a complex inflammatory process involving local glial and infiltrating immune cells that promote the upregulation of pro-inflammatory mediators responsible for the post-traumatic inflammatory cascade. Chronic microglial activation was found one year after moderate-to-severe contusion (Loane et al., 2014). Moreover, unresolved pro-inflammatory phenotype has been observed to persist chronically after moderate-to-severe TBI in both preclinical and clinical studies. Also, reactive oxygen species (ROS) and reactive nitrogen species (RNS) can act as key regulators of inflammatory signaling promoting the expression of various pro-inflammatory mediators (Morgan and Liu, 2011).

Despite several preclinical studies evaluating a plethora of pharmacological agents, there is currently no effective neuroprotective therapy or cure for individuals with TBI (Kokiko and Hamm, 2007; Kline et al., 2016; Margulies et al., 2016). The lack of translational success may be due to inappropriate dosing and/or temporal window. Given the paucity of therapeutic interventions for TBI, preclinical rehabilitative paradigms are gaining momentum as they may enable successful translation with minimal to no adverse side effects (Bondi et al., 2014; de la Tremblaye et al., 2019). Environmental enrichment (EE) is a multifaceted expansive housing environment consisting of multiple stimuli and social interaction that collectively yield a preclinical model of multimodal neurorehabilitation, which reliably provides behavioral and histological benefits after TBI independently of injury severity, age or sex (Bondi et al., 2014; de la Tremblaye et al., 2019). The diverse benefits induced by EE in TBI models have been attributed to various physiological and anatomical responses (Bondi et al., 2014). In uninjured control rats, EE promoted dendritic arborization and both cortical and hippocampal synaptogenesis (van Praag et al., 2000; Frick and Fernandez, 2003). EE increased the expression of brain-derived neurotrophic factor (BDNF) and fibronectin type III domain-containing protein 5 in the cerebral cortex of mice subjected to middle cerebral artery occlusion (Yu et al., 2020). Therefore, given that oxidative stress and neuroinflammatory responses are prominent secondary sequelae of TBI, we sought to evaluate whether the EE-induced behavioral and functional benefits correlate with attenuation of these deleterious effects.

2. Methods

2.1. Animals

Forty-eight (3-month-old) male Sprague-Dawley rats (Envigo RMS, Indianapolis, IN) were housed in pairs in standard (STD) laboratory ventilated polycarbonate cages in a temperature (21 ± 1 °C) and light-controlled (7:00 a.m. to 7:00 p.m.) vivarium with ad libitum food and water. After a week of acclimatization, the rats were pretrained on the designated motor tasks (see motor performance section for details) in preparation for surgery. The rats were randomly assigned to four groups of 12 in each: Sham + STD, Sham + EE, TBI + STD, and TBI + EE. A power analysis (G*power 3.1.9.4) indicated that an $n = 10$/group yields sufficient power (95%) for the behavioral assays. Despite the power analysis, we included an extra 2 rats in each group to account for possible attrition due to surgery or behavioral outliers. All experimental procedures were approved by the Institutional Animal Care and Use Committee at the University of Pittsburgh. Every attempt was made to limit the number of rats used and to minimize suffering. One rat from the TBI + STD group was excluded from the analyses because of an inability to locate the visible platform, which may be indicative of visual acuity deficits and therefore could be a potential confound given the necessity to see the cues located on the walls to acquire spatial learning.

2.2. Surgery

Controlled cortical impact (CCI) or Sham surgeries were performed as previously reported (Kline et al., 2002; Kline et al., 2010; Lajud et al., 2019; Moschonas et al., 2021). Briefly, the rats received a 4% concentration of isoflurane in 2:1 N_2O:O_2 for anesthetic induction, after which they were endotracheally intubated and secured on a stereotaxic frame. During mechanical ventilation, the carrier gases remained the same, but the concentration of isoflurane was reduced to 2%, which was sufficient for maintaining an adequate plane of surgical anesthesia. Core temperature was maintained at 37 ± 0.5 °C with the use of a heating pad and monitored with a rectal thermistor probe. Using aseptic procedures, a midline scalp incision was made followed by a craniectomy of approximately 8 mm in diameter in the right hemisphere. The impact tip (6 mm, flat) was centered through the craniectomy until it touched the dura mater and then it was advanced 2.8 mm farther and impacted the cortex at 4 m/s to cause a moderate-to-severe injury. Sham rats underwent similar surgical procedures but were not subjected to the impact. Anesthesia was discontinued immediately after the CCI injury, the incision was sutured, and the rats were extubated. Sham rats were sutured while under anesthesia. Rats were euthanized at 21 days after TBI or Sham injury.

2.3. Acute neurological evaluation

Immediately after the discontinuation of anesthesia, acute neurological outcomes were assessed. Briefly, limb reflex ability was determined by gently squeezing the left and right hind paw every 5 s and recording the withdrawal latency. Righting reflex was assessed by measuring the time required to turn from the supine to prone position on three consecutive trials. These acute tests are sensitive indicators of injury severity and anesthetic effects (Kline et al., 2010; de la Tremblaye et al., 2021).

2.4. Housing conditions

After recovery from anesthesia, as evidenced by spontaneous movement in the holding cage, the rats were returned to the colony where those designated for enrichment were immediately placed in the EE cages (Bondi et al., 2014; Moschonas et al., 2021). The EE cages (92 × 78 × 51 cm) were fabricated with stainless-steel wire mesh and included ladders that allowed the rats to ambulate all three levels. Contained in the EE cages were various toys (e.g., blocks, tubes, balls), nesting materials (e.g., bedding) and ad libitum food and water. To maintain novelty, the objects were rearranged daily, and the cages were cleaned twice per week. To minimize variability, 10–12 rats (TBI and Sham) were housed together. Rats assigned to STD housing were placed as pairs in ventilated polycarbonate cages (37 × 25 × 18 cm) with only ad libitum food and water.

2.5. Motor performance

Motor function was assessed with beam-balance and beam-walk tasks that have been extensively used in the neurotrauma field and in our laboratory (Kline et al., 2002; Bao et al., 2019). The beam-balance task consists of placing a rat on an elevated (90 cm) narrow (1.5 cm wide) wooden beam and recording the time it remains on for a maximum of 60 s. The beam-walk task consists of training rats to escape a bright light and white noise (i.e., negative reinforcement) by traversing an elevated narrow beam (2.5 cm wide x 100 cm long) and entering a darkened goal box. Beam-walk performance was assessed by recording the elapsed time to traverse the beam as well as the distance traveled using scoring criteria based on a rating scale from 0 to 5 where 0 indicates an inability to ambulate beyond the start point and 5 indicates walking down the entire beam and entering the goal box. Prior to surgery, all rats were trained to maintain balance for 60 s and traverse the beam in under 5 s, which typically required 3–5 trials. Baseline performance was assessed on the day of surgery. On post-operative days 1–5, the rats were tested on both motor tasks and given three 60 s trials per day on each task. Daily scores were averaged for each rat and used in the statistical analyses.

2.6. Cognitive performance

Spatial learning and memory retention were assessed using a well-established Morris water maze (MWM) task that is sensitive to cognitive function/dysfunction after TBI (Kline et al., 2002; Kline et al., 2010). Briefly, the maze consists of a plastic pool (180 cm diameter; 60 cm high) filled with water (26 ± 1 °C) to a depth of 28 cm with salient visual cues that remained constant throughout the study. The escape platform, a clear Plexiglass stand (10 cm diameter, 26 cm high), was positioned 26 cm from the maze in the southwest quadrant and held constant for each rat. Spatial learning, represented by the ability to locate the submerged (2 cm below the water surface) escape platform began on post-operative day 14 and consisted of providing a block of four daily trials with a 4-min inter-trial-interval (ITI) for five consecutive days (i.e., 14–18). For each daily block of trials, the rats were placed in the pool facing the wall at each of the four possible start locations in a randomized manner. Each trial lasted until the rat climbed onto the platform or until 120 s elapsed. The rats remained on the platform for 30 s before being placed in a heated incubator during the 4 min ITI. The times of the four daily trials for each rat were averaged and used in the statistical analysis.

On post-operative day 19, both memory retention and visible platform tests were conducted. Memory retention was carried out before the visible platform test so as not to provide a refresher for platform location, and consisted of a single probe trial where the platform was removed, and the rats were given the opportunity to explore the pool for 30 s. The more time the rats spent searching for the platform in the quadrant where it was previously situated (i.e., target quadrant) was indicative of better memory retention. Following the probe trial, the platform was raised 2 cm above the water surface to determine non-spatial factors on cognitive performance or visual acuity deficits. The data, which included time to locate the submerged and visible platform, time in the target quadrant, and swim speed were obtained using video tracking software.

2.7. Immunohistochemistry

Three weeks after CCI injury or sham surgery, the rats were anesthetized with Fatal-Plus (0.3 mL, i.p.) and perfused transcardially with 200 mL of 0.1 M of phosphate-buffered saline (pH 7.4) followed by 300 mL of 4% paraformaldehyde (PFA). The brains (4 in each group) were post-fixed in 4% PFA for 7 days and then placed in 30% sucrose in PBS until infiltration was complete (~3 days), then flash-frozen in liquid nitrogen and stored in −80 °C until ready to cut. The brains were cut coronally using a cryostat microtome at 35 μm, and the sections were stored in cryoprotectant at −20 °C until ready for immunohistochemistry. Unless otherwise specified, all incubations were carried out at room temperature (RT).

Brain sections were washed 3 × 10 min in PBS and pre-incubated for 5 h with 1% Triton X-100 in PBS at 4 °C. The tissue was washed again (3 × 10 min) followed by 5 min at 37 °C for the antigen retrieval step (Invitrogen Life Technologies; Carlsbad, CA, USA). Next, the sections were blocked for 1 h. An antibody against microtubule-associated protein 2 (chicken MAP2; 1:2000, Millipore) was used to label neuronal cell bodies and dendrites and to study their cytoskeleton structure. In combination with other antibodies, MAP2 staining allows detection of potential changes in the immunoreactivity of proteins between neurons (pyramidal) and the neuropil. To evaluate oxidative damage, hippocampal sections were incubated for 72 h at 4 °C with antibodies against mouse 4-HNE (1:500, Percipio Biosciences) or rabbit 3-NT (1:500, Millipore). To investigate the neuroinflammatory response in the hippocampus, sections were incubated for 72 h at 4 °C with rabbit ionized calcium-binding adapter molecule (Iba1; 1:25000, Wako) primary antibody. To assess the hippocampal immunoreactivity of the *N*-methyl-D-aspartate receptor 1 (NMDAR1), brain sections were incubated for 72 h at 4 °C with a rabbit NMDAR1 (1:1000, Abcam) antibody.

After incubation, the tissue was rinsed (3 × 10 min) in PBS and incubated in a secondary antibody, which for neuroinflammation was anti-mouse Alexa Fluor 647-conjugated IgG (1:500, Life Technologies) and anti-rabbit Cy3 543-conjugated IgG (1:500, Jackson Immuno Research), while for oxidative stress it was anti-chicken DyLight 405-conjugated IgG (1:500, Jackson Immuno Research) and anti-rabbit Cy3 543-conjugated IgG (1:500, Jackson Immuno Research) for 2 h. After 3 PBS washes of 10 min each, the sections were mounted onto plus coated glass slides and cover slipped using gelvatol mounting medium. Combined CA1 and CA2 regions of the hippocampus ipsilateral and contralateral to injury were examined using confocal laser microscopy. Quantitative analyses of markers were carried out in three sections per rat (n = 4 group).

2.8. Confocal laser microscopy

Confocal laser microscopy was used to evaluate oxidative damage and the pro-inflammatory response as well as variations in the immunoreactivity of NMDAR1. Images of the stained rat brain sections were acquired on an Olympus BX61 Fluoview 1000 under constant power and pinhole aperture with a 20× (N.A. 0.75) lens. Quantification was carried out using the Fluoview Viewer Olympus software (v. 4.2c). Final fluorescence micrographs were obtained using a PlanApo 60× oil-immersion objective (1.45 N.A.) at high resolution (100 μs).

2.9. Microglial activation

Rat hippocampal sections were immunolabeled using an antibody against the Iba1 epitope. Fluorescent micrographs were acquired using a confocal microscope at 20× (N.A. 0.75). Digital pictures were exported and analyzed using the Fiji software (ImageJ, v1.52). RGB color images were converted into 8-bit grayscale files with pixel values ranging from 0 to 255. After creating a region of interest, background was subtracted, and the average pixel intensity was determined. Values for the number of microglial-positive cells were generated.

2.10. Data analyses

Statistical analyses were conducted on data collected by researchers blinded to group conditions using StatView 5.0.1 software (Abacus Concepts, Inc., Berkeley, CA). The motor and cognitive data were ana-

lyzed by repeated-measures analysis of variance (rmANOVA). Acute neurological assessment, probe trial, visible platform, and swim speed were analyzed by two-way ANOVAs with housing and injury as factors. Quantification of Iba1, 3-NT, 4-HNE, and NMDAR1 immunoreactivity was assessed by ANOVAs. The Newman-Keuls multiple comparisons post-hoc test determined specific group differences. The results are expressed as the mean ± standard error of the mean (S.E.M.). $p < 0.05$ was considered significant. For correlation analysis, entire data sets for each variable (i.e., all rats) were tested with the Shapiro-Wilk test for normal distribution and a correlation analysis was estimated. A heat map was obtained for Spearman's correlation coefficients.

3. Results

3.1. Acute neurological evaluation

No significant differences were observed between the TBI groups for return of hind limb reflex ability after a brief paw pinch (mean range for right = 168.7 ± 3.1 s to 187.9 ± 10.8 s; mean range for left = 172.5 ± 3.3 s to 191.0 ± 10.6 s) or righting reflex latency (mean range = 416.6 ± 16.4 s to 428.8 ± 15.9 s) after cessation of anesthesia ($p > 0.05$). The lack of significant differences in post-surgical neurological assessments between the TBI groups indicates that all rats received an equivalent level of injury and anesthesia. Also, no differences were found between the Sham groups ($p > 0.05$) in hind limb reflex (mean range for right = 33.9 ± 7.1 s to 37.9 ± 5.1 s; mean range for left = 37.5 ± 7.4 s to 41.1 ± 4.9 s) or righting reflex (mean range = 116.8 ± 6.8 s to 119.7 ± 5.5 s).

3.2. Motor performance

3.2.1. Beam-balance

Baseline performance prior to surgery revealed that every rat was able to balance on the beam for the allotted 60 s (Fig. 1A). Following TBI, the rmANOVA showed significant Group ($F_{3,43} = 17.535$, $p < 0.0001$) and Day ($F_{5,215} = 21.327$, $p < 0.0001$) differences, as well as a significant Group x Day interaction ($F_{15,215} = 7.665$, $p < 0.0001$). The post-hoc analysis indicated that both TBI groups (EE and STD) were significantly impaired relative to the Sham groups ($p < 0.05$), which were able to maintain baseline-level balance through the 5 days of testing and did not differ from one another ($p > 0.05$). Between the brain injured groups, TBI + EE performed markedly better than TBI + STD ($p < 0.05$).

3.2.2. Beam-walk time

No pre-surgical differences in time to traverse the beam were observed among the groups as all rats were well-trained and proficiently reached the goal box in under 5 s (Fig. 1B). After TBI, the rmANOVA showed significant Group ($F_{3,43} = 214.179$, $p < 0.0001$) and Day ($F_{5,215} = 208.378$, $p < 0.0001$) differences, as well as a significant Group x Day interaction ($F_{15,215} = 61.983$, $p < 0.0001$). The post-hoc analysis demonstrated that both TBI groups (EE and STD) were significantly impaired relative to the Sham groups ($p < 0.05$), which were able to maintain baseline-level traversal times through the 5 days of testing and did not differ from one another ($p > 0.05$). Between the brain injured groups, TBI + EE performed better than TBI + STD ($p < 0.05$).

3.3. Beam-walk score

Baseline performance prior to surgery indicated that every rat was able to traverse the entire length of the beam and enter the goal box for a maximum score of 5 (Fig. 1C). Following TBI, the rmANOVA showed significant Group ($F_{3,43} = 80.722$, $p < 0.0001$) and Day ($F_{5,215} = 74.018$, $p < 0.0001$) differences, as well as a significant Group x Day interaction ($F_{15,215} = 25.889$, $p < 0.0001$). The post-hoc analysis showed that both TBI groups (EE and STD) were significantly impaired relative to the Sham groups ($p < 0.05$), which were able to maintain baseline-level performance through the 5 days of testing and did not differ from one another ($p > 0.05$). Between the brain injured groups, TBI + EE performed markedly better than TBI + STD having reached baseline performance by the end of the testing period ($p < 0.05$).

3.4. Cognitive performance

3.4.1. Spatial learning

Analysis of the spatial learning data showed significant Group ($F_{3,43} = 69.644$, $p < 0.0001$) and Day ($F_{4,172} = 25.532$, $p < 0.0001$) differences (Fig. 2A). The post-hoc test demonstrated that the TBI + EE group located the escape platform significantly quicker over time vs. the TBI + STD group ($p < 0.05$). There was no difference between the Sham groups regardless of housing (STD vs. EE), but both were better at locating the escape platform relative to both TBI groups ($p < 0.05$). No differences in time to locate the visible platform (mean range = 23.8 ± 2.0 s to 31.1 ± 1.9 s) or swim speed (mean range = 28.3 ± 1.2 cm/s to 32.3 ± 1.8 cm/s) were observed among

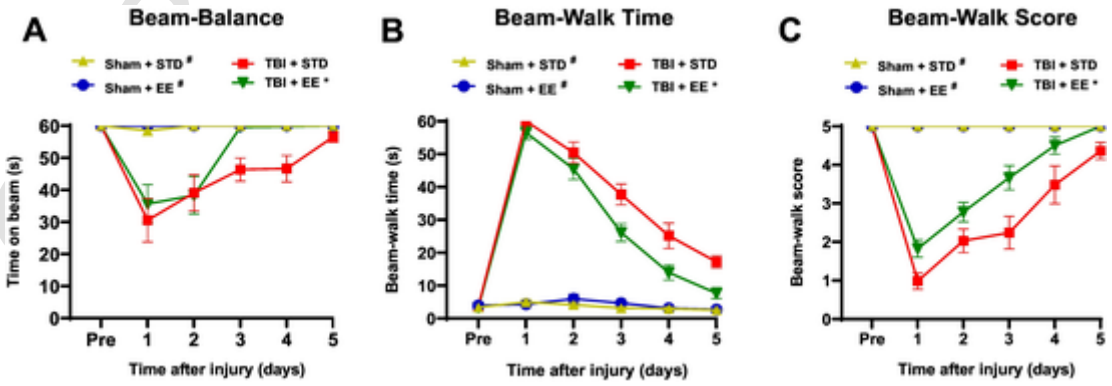

Fig. 1. Motor performance. (A) Time (s) to maintain balance on an elevated narrow beam prior to, and after, TBI or Sham injury on post-operative days 1–5. $^{\#}p < 0.05$ vs. TBI + STD and TBI + EE and $^{*}p < 0.05$ vs. TBI + STD. No statistical difference was revealed between the Sham groups. (B) Time (s) to traverse an elevated narrow beam prior to, and after, TBI or sham injury on post-operative days 1–5. $^{\#}p < 0.05$ vs. TBI + STD and TBI + EE and $^{*}p < 0.05$ vs. TBI + STD. No statistical difference was revealed between the Sham groups. (C) Distance traveled along an elevated narrow beam prior to, and after, TBI or sham injury on post-operative days 1–5. $^{\#}p < 0.05$ vs. TBI + STD and TBI + EE and $^{*}p < 0.05$ vs. TBI + STD. No statistical difference was revealed between the Sham groups. All data were analyzed by repeated measures ANOVA followed by the Newman-Keuls multiple comparisons post-hoc test. The results are expressed as the mean ± S.E.M.

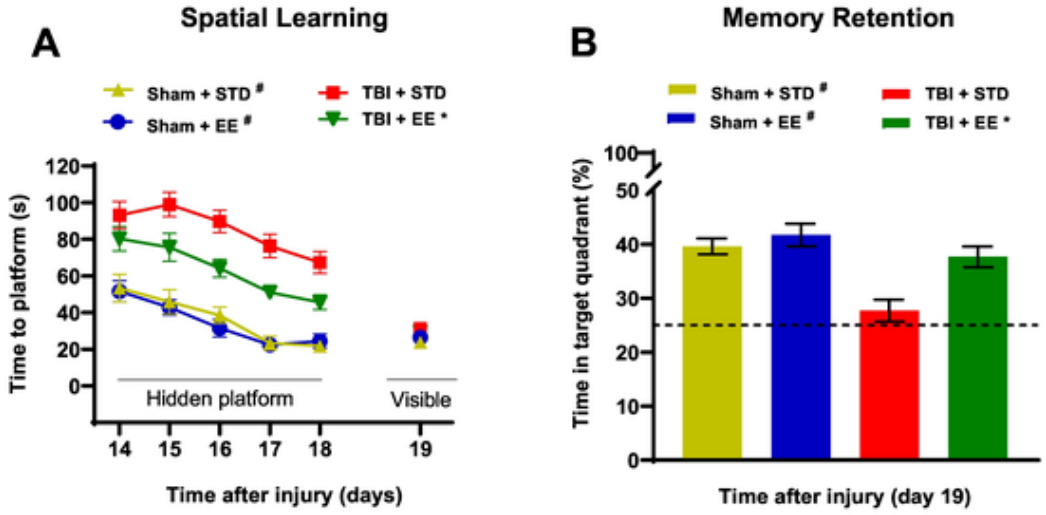

Fig. 2. Cognitive performance. (A) Time (s) to locate a submerged (i.e., hidden) and visible platform in the Morris water maze on post-operative days 14–19. $^{\#}p < 0.05$ vs. TBI + STD and TBI + EE and $^{*}p < 0.05$ vs. TBI + STD. No statistical difference was revealed between the Sham groups. No differences were noted among the groups in time to locate the visible platform ($p > 0.05$). (B) Percent of time spent in the target quadrant (i.e., where the platform was previously located) following a single probe trial at day 19. $^{\#}p < 0.05$ vs. TBI + STD and $^{*}p < 0.05$ vs. TBI + STD. No statistical differences were revealed among the TBI + EE, Sham + STD, and Sham + EE groups ($p > 0.05$). Dotted line represents performance at the chance level (25%). All data were analyzed by repeated measures ANOVA followed by the Newman-Keuls multiple comparisons post-hoc test. The results are expressed as the mean ± S.E.M.

the groups suggesting there were no extraneous factors precluding the accurate assessment of spatial learning.

3.4.2. Memory retention

Analysis of the probe data exhibited a significant Group effect ($F_{3,43} = 10.226$, $p < 0.0001$; Fig. 2B). The post-hoc analysis confirmed significant memory retention in the Sham + EE, Sham + STD, and TBI + EE groups as evidenced by a greater percentage of the allotted time spent in the target quadrant (41.7 ± 2.1%, 39.6 ± 1.4%, and 37.6 ± 1.9%, respectively) vs. the TBI + STD group (27.7 ± 2.0%). No significant differences were found between the Sham controls (EE and STD) or among the Shams and the TBI + EE group ($p > 0.05$).

3.5. Protein nitration

Oxidative stress, including damage to proteins, is a major contributor to secondary injury signaling cascades following TBI. Protein tyrosine nitration was assessed in the rat brain (Fig. 3). The ANOVA showed significant Group differences in the ipsilateral ($F_{3,20} = 32.15$, $p < 0.0001$) and contralateral ($F_{3,20} = 12.11$, $p < 0.0001$) hippocampal CA1/CA2 regions. Post-hoc analyses revealed significant 3-NT immunoreactivity in the TBI groups relative to the Sham + STD controls in both hemispheres. A significant reduction of 3-NT immunoreactivity was noted in the TBI + EE group vs. the TBI + STD group ipsilateral to the injury ($p < 0.05$) but not contralateral ($p > 0.05$). Moreover, the TBI + EE group did not differ from the Sham + EE group in the ipsilateral hippocampus ($p > 0.05$). Lastly, there was no difference between the Sham groups regardless of the hemisphere ($p > 0.05$).

3.6. Lipid peroxidation

The pathophysiology of TBI is complex and involves multiple and complex signaling cascades, including LPO, which plays a critical role in in cell membrane damage and concomitant cell death, including apoptosis. Therefore, we examined whether EE showed beneficial antioxidant effects in TBI rats. Damage to lipids was quantified by measuring the immunofluorescence signal of 4-HNE (Fig. 4). Group differences in the ipsilateral ($F_{3,20} = 14.04$, $p < 0.0001$) and contralateral ($F_{3,20} = 5.444$, $p = 0.0067$) were described in the hippocampal CA1/CA2 regions. Post-hoc analyses showed significant 4-HNE immunoreactivity in the TBI groups relative to the Sham + STD controls in both hemispheres. A significant reduction of 4-HNE immunoreactivity was observed in the TBI + EE group vs. the TBI + STD group in the ipsilateral ($p < 0.05$) but not in the contralateral hippocampus ($p > 0.05$). No differences were observed between the TBI + EE and the Sham + EE groups in the contralateral hippocampus ($p > 0.05$). No changes were found between the Sham groups independently of the hemisphere ($p > 0.05$).

3.7. Microglial activation

As activated microglia are a hallmark of TBI, we determined the extent by which EE could attenuate the injury-induced neuroinflammatory response in a rat model of TBI. Activated microglial cells were detected using the Iba1 marker (Fig. 5). Robust Group differences were seen in the ipsilateral ($F_{3,23} = 21.89$, $p < 0.0001$) and contralateral ($F_{3,23} = 7.606$, $p = 0.0010$) hippocampus. Post hoc analysis showed no differences between the STD-and EE-housed Sham groups in either hemisphere. The TBI + STD group had significantly greater Iba1 immunoreactivity compared to the TBI + EE group in both hemispheres.

3.8. NMDA receptor 1

The levels of extracellular glutamate are robustly increased following TBI, resulting in an excessive NMDAR activation. Thus, the immunoreactivity of NMDAR1 was determined in the rat brain (Fig. 6). The ANOVA analysis displayed significant Group differences in the ipsilateral ($F_{3,23} = 25.14$, $p < 0.0001$) and contralateral ($F_{3,24} = 12.47$, $p < 0.0001$) hippocampal CA1/CA2 regions. Post-hoc analyses revealed that both TBI groups had elevated NMDAR1 immunoreactivity relative to both Sham controls in the ipsilateral hippocampus, but only the TBI + STD group exhibited an increase in NMDAR1 fluorescence signal in the contralateral hippocampus. The data further showed that NMDAR1 immunoreactivity was reduced in the TBI + EE group vs. the TBI + STD group in both hemispheres.

3.9. Correlation analysis

Spearman's correlation analysis (Fig. 7) indicated that 3-NT and 4-HNE correlated with behavior ($r > 0.4$ or $r < -0.4$, $p < 0.05$). Also, a

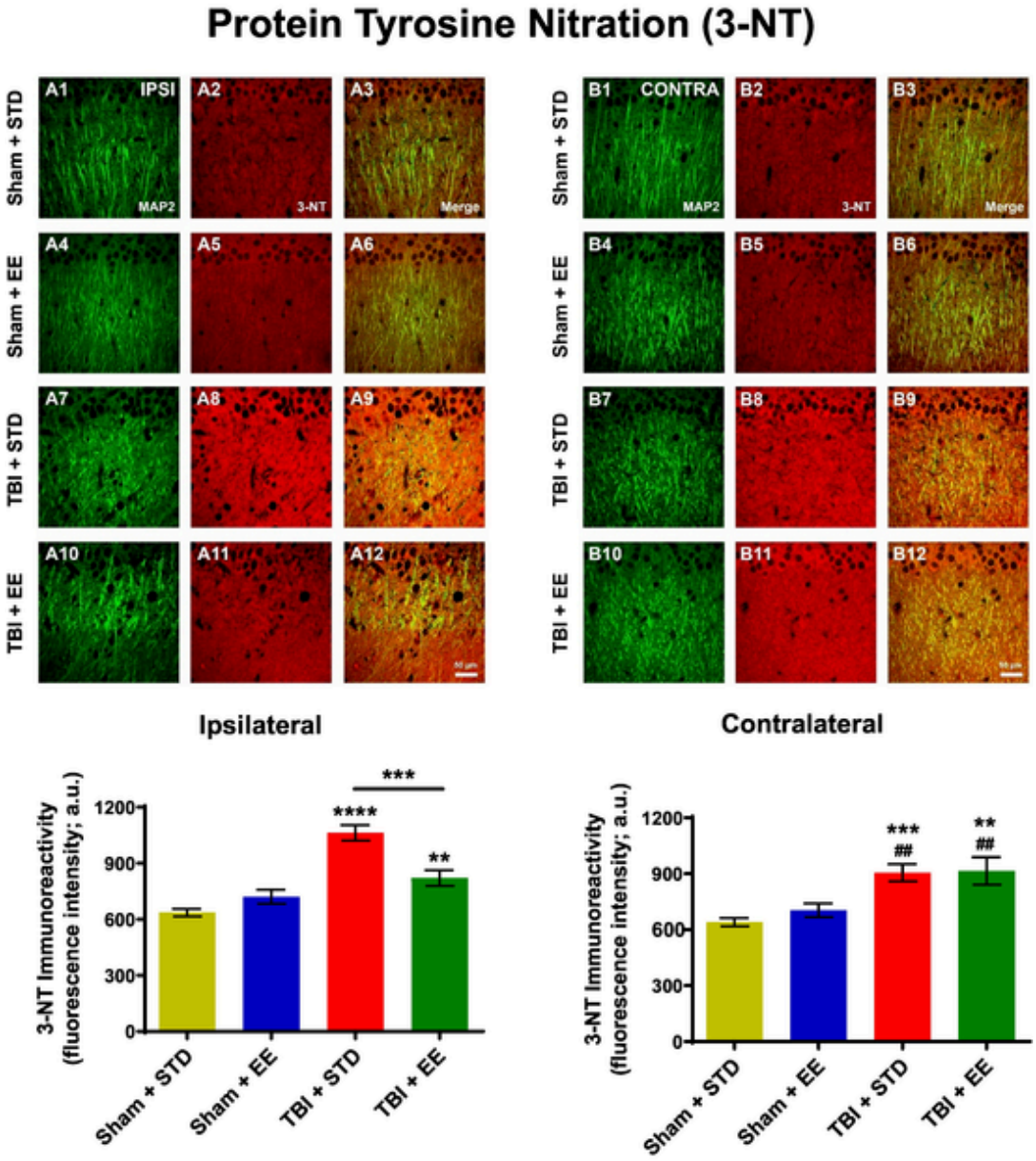

Fig. 3. Protein nitration. Quantification of 3-NT immunofluorescence signal was carried out in the rat ipsilateral and contralateral hippocampus on post-operative day 21. Data were analyzed by ANOVA followed by the Newman-Keuls multiple comparisons post-hoc test to determine specific group differences. The results are expressed as the mean ± S.E.M. In the hippocampus ipsilateral to TBI or Sham surgery, $^{**}p < 0.01$ vs. Sham + STD; $^{***}p < 0.001$ vs. TBI + STD; $^{****}p < 0.0001$ vs. Sham + STD and Sham + EE. No difference was revealed between the TBI + EE and Sham + EE ($p > 0.05$). In the hippocampus contralateral to TBI or Sham surgery, $^{**}p < 0.01$ vs. Sham + STD; $^{***}p < 0.001$ vs. Sham + STD; $^{\#\#}p < 0.01$ vs. Sham + STD and Sham + EE. No difference was observed between the Sham groups in either hemisphere ($p > 0.05$). Scale bar = 50 μm.

significant correlation was observed for Iba1 immunoreactivity from the ipsilateral hippocampus that was more robust that for the contralateral. The strongest correlations with behavior were observed for NMDAR1 immunoreactivity from the ipsilateral hemisphere ($r > 0.6$ or $r < -0.6$, $p < 0.0001$). The results indicate a positive correlation for NMDAR1 immunofluorescence with the time to traverse the beam and escape latency during the five days of the learning phase of MWM (r26 > 0.50, $p < 0.01$). NMDAR1 immunofluorescence negatively correlated with the time in the beam-balance test and the score in the beam-walk test (r26 < −0.50, $p < 0.01$). Also, NMDAR1 expression from the ipsilateral hippocampus positively correlated with 3-NT (r23 = 0.82, $p < 0.0001$), 4-HNE (r23 = 0.82, $p < 0.0001$), and Iba1 immunoreactivity (r26 = 0.78, $p < 0.0001$). Note that while 3-NT, 4-HNE, and NMDAR1 immunoreactivity correlated with spatial learning, only Iba1 immunoreactivity showed a significant correlation with memory retention, and this effect was stronger for the contralateral hemisphere (r26 = −0.50, $p < 0.01$) relative to the ipsilateral hemisphere (r26 = −0.42, $p < 0.05$).

4. Discussion

After TBI, complex secondary pathogenic sequelae such as widespread free radical overproduction and microglial activation initiate abnormal cellular and molecular dysfunction that yields progressive neurodegeneration and behavioral deficits (Block et al., 2007; Hill et al., 2017). The aim of the current study was to investigate the neuroprotective effects of EE, and more specifically, whether EE would prevent biochemical failures and improve functional recovery in a rat CCI model of TBI. The severity of injury in TBI is directly associated with ROS-induced tissue damage (Di Pietro et al., 2014). Nitration of tyrosine

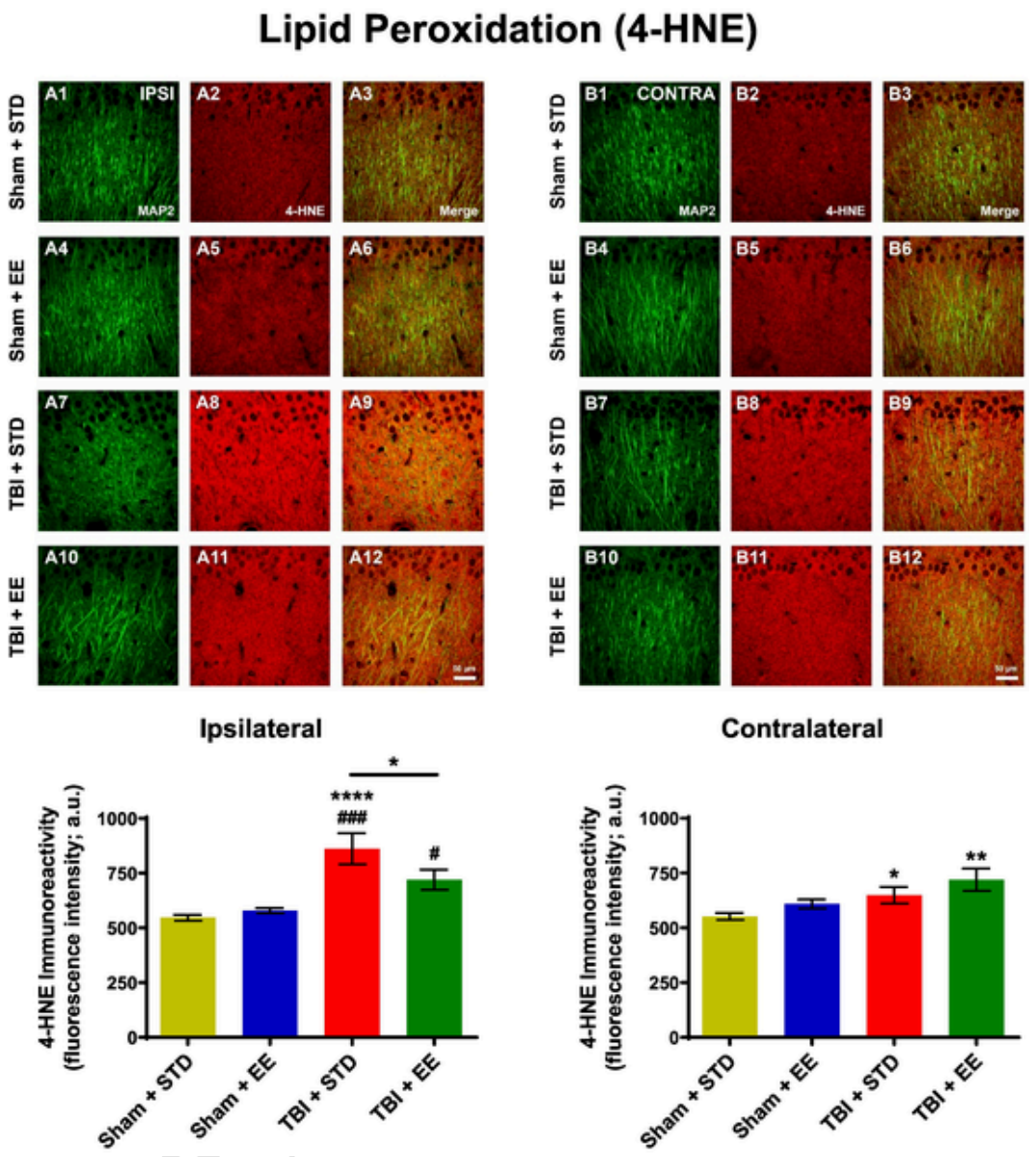

Fig. 4. Lipid peroxidation. Quantification of the fluorescence intensity of 4-HNE was assessed in the rat ipsilateral and contralateral hippocampus was performed at 3 weeks post-injury. Data were analyzed by ANOVA followed by the Newman-Keuls multiple comparisons post-hoc test. The results are expressed as the mean ± S.E.M. In the hippocampus ipsilateral to TBI or Sham surgery, $^{*}p < 0.05$ vs. TBI + STD; $^{****}p < 0.0001$ vs. Sham + STD; $^{\#}p < 0.05$ vs. vs. Sham + STD and Sham + EE; $^{\#\#\#}p < 0.001$ vs. Sham + EE. In the hippocampus contralateral to TBI or Sham surgery, $^{*}p < 0.05$ vs. Sham + STD; $^{**}p < 0.01$ vs. Sham + STD. No differences were revealed among the TBI + STD, TBI + EE, and Sham + EE groups ($p > 0.05$). No difference was observed between the Sham groups in either hemisphere ($p > 0.05$). Scale bar = 50 μm.

residues can regulate changes in protein structure and function, thereby affecting cell homeostasis. Aberrant protein nitration has been observed in individuals with TBI and in experimental animal models (Darwish et al., 2007; Deng et al., 2007; Readnower et al., 2010). Increased neuronal and glial 3-NT immunoreactivity was found in the CSF of TBI patients (Darwish et al., 2007). Peroxynitrite ($ONOO^{-}$) and 3-NT mediate nitrosative stress damage in a model of severe CCI focal TBI, contributing to an excessive Ca^{2+} accumulation, cytoskeletal degradation, and neurodegenerative processes (Deng et al., 2007). The number of 3-NT-positive neurons was increased in the mouse cortex and hippocampus after concussive brain injury (Miyamoto et al., 2013; Higashi et al., 2014). Our results showed a significant correlation of the expression of hippocampal 3-NT levels with motor and cognitive performance.

Peroxidation of lipid species can alter the biological membrane function and properties (e.g., permeability and fluidity), induce free radical damage, and promote mitochondrial dysfunction. Following TBI, oxidative stress is prominently manifested as LPO in neurons and glial cells. Elevated levels of MDA and 8-isoPGF2α within 6 h were detected in the ipsilateral cortex of TBI rats (Ji et al., 2010). The concentration of MDA was markedly augmented in the brain samples of TBI rats (Solaroglu et al., 2005). Oxidation-mediated lipid damage was seen in a unilateral CCI model of TBI (Sullivan et al., 1998). The number of 4-HNE^{+} cells was elevated in the rat cerebral cortex three days after inflicting TBI (Itoh et al., 2009). We found a significant increase in 3-NT and 4-HNE immunoreactivity in the rat ipsilateral hippocampus, which was reduced by EE. These alterations significantly correlated with motor performance and spatial learning.

A direct relationship between 3-NT and 4-HNE has been described in TBI. RNS (mainly $ONOO^{-}$) are considered a major player in TBI-induced oxidative insult. $ONOO^{-}$decomposes into highly reactive free radicals that trigger membrane LPO of polyunsaturated fatty acids and protein nitration. In addition, LPO results in the formation of toxic alde-

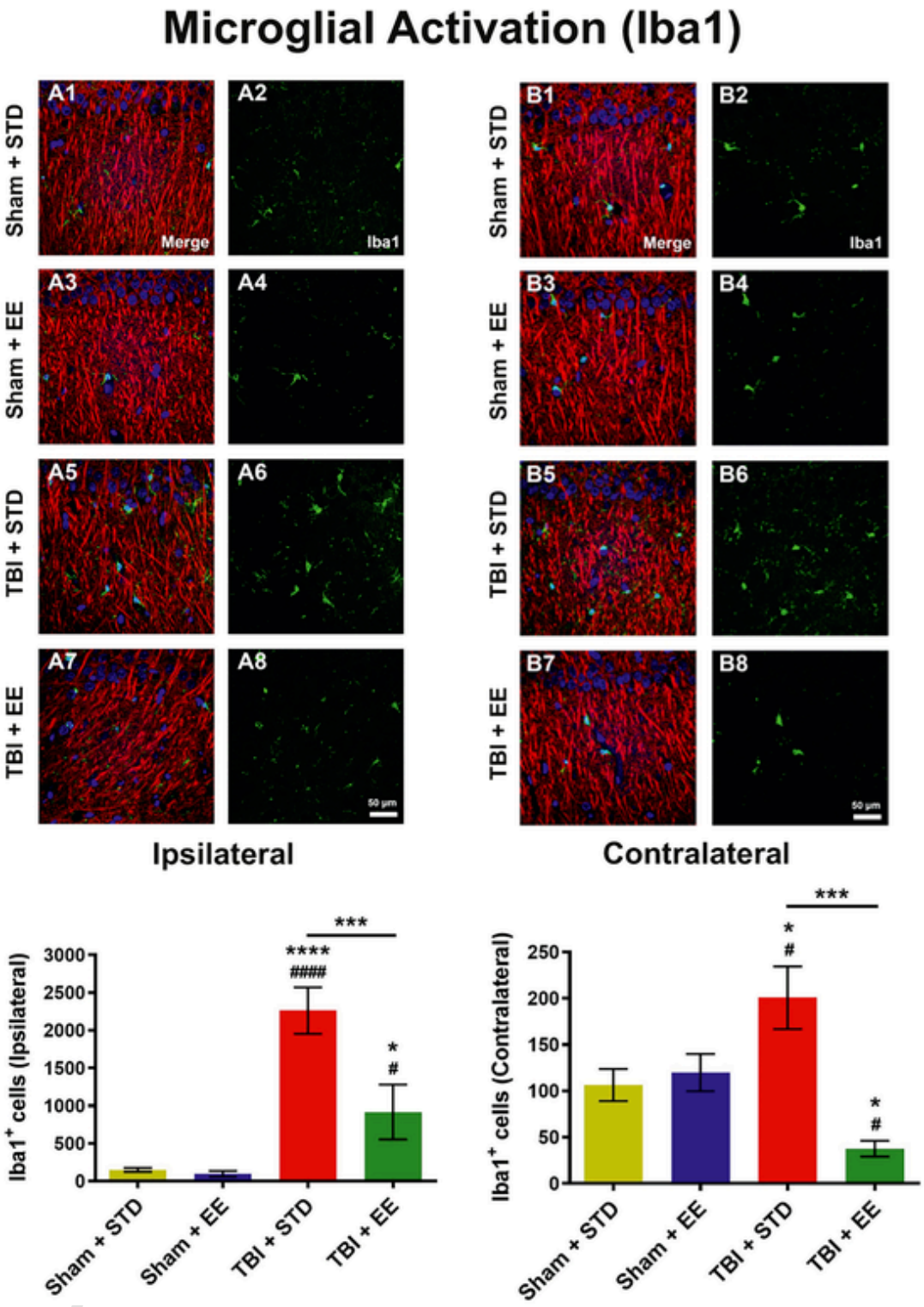

Fig. 5. Microglial activation. Iba1-immunoreactive cells were quantitated in both the ipsilateral and the contralateral sides of rat hippocampus on post-operative day 21. Data were analyzed by ANOVA followed by the Newman-Keuls multiple comparisons post-hoc test to determine specific group differences. The results are expressed as the mean ± S.E.M. In the hippocampus ipsilateral to TBI or Sham surgery, $^{*}p < 0.05$ vs. Sham + STD and Sham + EE; $^{***}p < 0.001$ vs. TBI + STD; $^{****}p < 0.0001$ vs. Sham + STD and Sham + EE. In the hippocampus contralateral to TBI or Sham surgery, $^{*}p < 0.05$ vs. Sham + STD and Sham + EE; $^{***}p < 0.001$ vs. TBI + STD; $^{\#}p < 0.05$ vs. Sham + STD and Sham + EE. No difference was detected between the Sham groups in either hemisphere ($p > 0.05$). Scale bar = 50 µm.

hyde byproducts, including 4-HNE and acrolein, that in turn, exacerbate ROS/RNS formation and oxidative damage to proteins. Hill and colleagues showed that time courses of 3-NT and 4-HNE were similar, with a peak after 48-72 h following CCI-TBI (Hill et al., 2017). More-

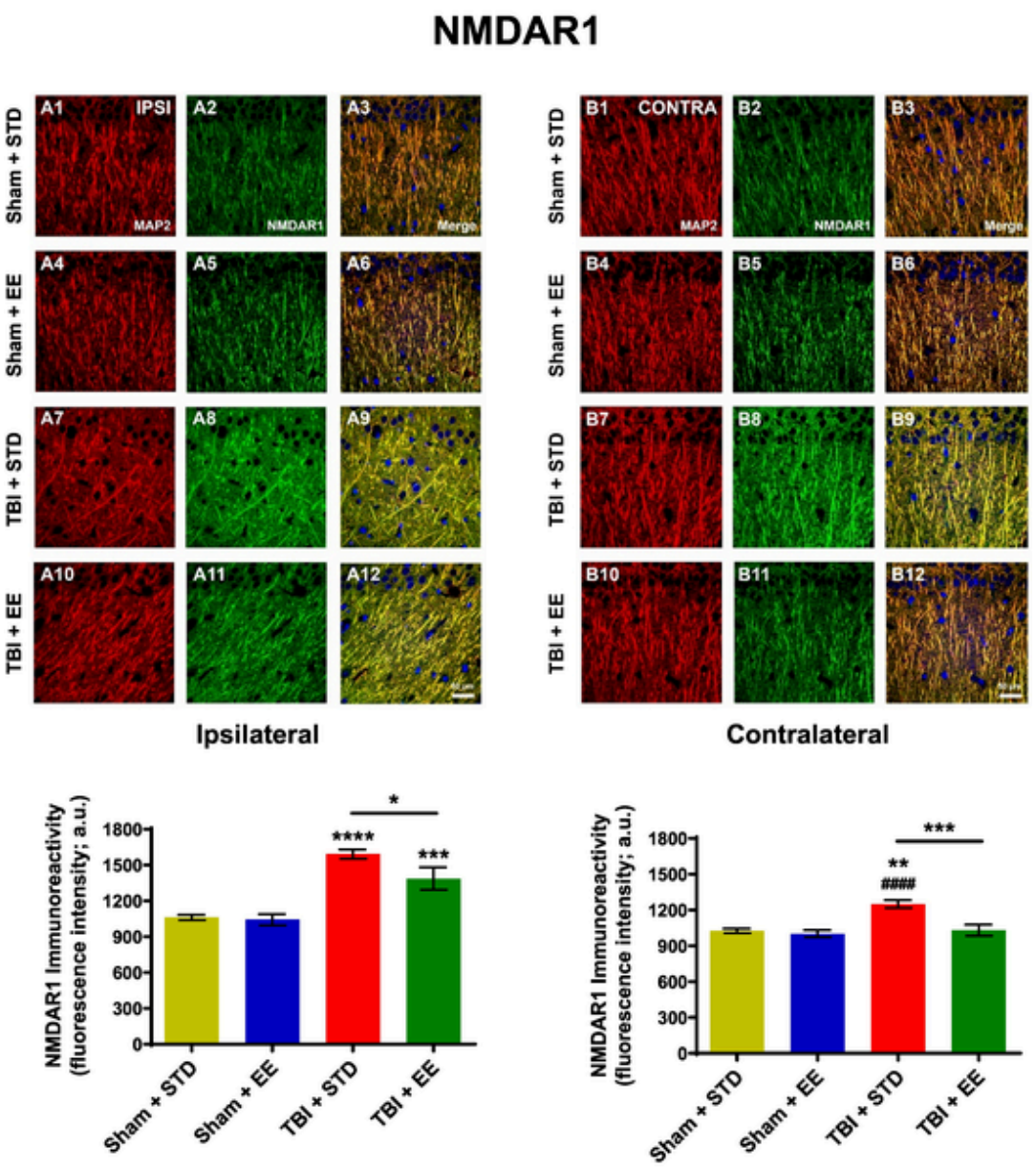

Fig. 6. NMDAR1 activation. NMDAR1 content was determined in the rat ipsilateral and contralateral hippocampus. Data were analyzed by ANOVA followed by the Newman-Keuls multiple comparisons post-hoc test and the results are expressed as the mean ± S.E.M. In the hippocampus ipsilateral to TBI or Sham surgery, $*p < 0.05$ vs. TBI + STD; $***p < 0.001$ vs. Sham + STD and Sham + EE; $****p < 0.0001$ vs. Sham + STD and Sham + EE. In the hippocampus contralateral to TBI or Sham surgery, $**p < 0.01$ vs. Sham + STD; $***p < 0.001$ vs. TBI + STD; $\#\#\#\#p < 0.0001$ vs. Sham + EE. No differences were revealed between the TBI + EE vs. Sham + STD and Sham + EE groups ($p > 0.05$). No difference was observed between the Sham groups in either hemisphere ($p > 0.05$). Scale bar = 50 μm.

over, a temporal and spatial relationship between $ONOO^-$-mediated oxidative insult, cytoskeletal degradation, and neurodegeneration was observed following TBI (Deng et al., 2007).

A prominent pro-inflammatory phenotype persists chronically after a moderate-to-severe TBI, in both clinical and pre-clinical studies (Ramlackhansingh et al., 2011; Loane et al., 2014; Coughlin et al., 2017). Clinically, PET studies demonstrated that (i) repeated TBI led to sustained glial activation in the brain of NFL players (Coughlin et al., 2017), and (ii) microglial stimulation can last up to 17 years in individuals with TBI (Ramlackhansingh et al., 2011). Pre-clinical studies have shown a prolonged microglial activation in the mouse cerebral cortex up to 1 year post-injury (Loane et al., 2014). This unresolved inflammation could be related to motor and cognitive impairments in the long term (Diaz-Chavez et al., 2020). In our study, Iba1 immunoreactivity was the only parameter that showed significant negative correlations with memory retention, thereby suggesting that microglial activation during the chronic phase of TBI predicts for more severe memory deficits. Memory impairment and executive functioning deficits are prominent symptoms following TBI (Wolf and Koch, 2016). Brain injury causes a disruption of brain structure and function that, combined with the pathophysiological changes related to aging, can exacerbate cognitive decline (Moretti et al., 2012). Cognitive impairment could be mediated, in part, by increased free radical generation and inflammation after TBI (Sun et al., 2019; Knopp et al., 2020. While several pre-clinical studies have demonstrated that antioxidant and anti-inflammatory pharmacotherapies ameliorate TBI-induced biochemical and neurobehavioral deficits, to date clinical trials have not yet conferred improvements, suggesting that alternative therapeutic interventions need to be elucidated (Hall et al., 2010; Mallah et al., 2020).

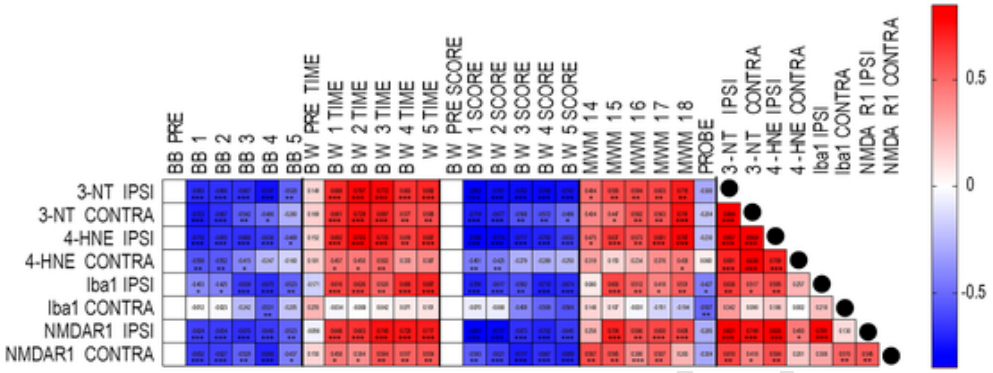

Fig. 7. Correlation analysis. Color heat map of the Spearman's correlation coefficients computed for the time on the beam-balance (BB), time to traverse the beam (BW TIME), beam-walk score (BW SCORE), escape latency, and percent of time in the target quadrant during the probe trial of the Morris water maze (MWM) with hippocampal 3-NT, 4-HNE, Iba1, and NMDAR1. Correlation coefficients are shown with continuous gradient colors where positive correlation is marked in red ($r > 0.4$, $*p < 0.05$; $r > 0.5$, $**p < 0.01$; and $r > 0.6$, $***p < 0.001$), negative is in blue ($r > -0.4$, $*p < 0.05$; $r > -0.5$, $**p < 0.01$; and $r > -0.6$, $***p < 0.001$), and white represents no correlation ($r = 0$, $p = 1$). (For interpretation of the references to color in this figure legend, the reader is referred to the web version of this article.)

Growing evidence has shown that EE promotes functional and cognitive recovery after TBI. It has been described that EE-mediated effect in restoring injury-induced motor deficits is attributed to the EE arena size, which allows increased ambulation across various surfaces and inclines as well as social components and stimulating objects (Sozda et al., 2010). Exposure of TBI rats to EE combined with targeted early-onset stimulation resulted in the recovery of neuromotor and cognitive dysfunction (Maegele et al., 2005). TBI-induced deficits on spatial memory and sensory discrimination were significantly reduced in EE exposed rats (Johnson et al., 2013). Following severe TBI, EE ameliorated functional outcome in adult rats (Passineau et al., 2001). Our laboratory has shown that abbreviated EE conferred neurobehavioral benefits, including spatial learning and memory recovery, and reduced cortical lesion volume in both male and female rats (de Witt et al., 2011; Radabaugh et al., 2016). EE also improved spatial learning and memory and mitigated the loss of medial septal and choline acetyltransferase neurons after CCI injury (Moschonas et al., 2021).

The mechanisms by which EE attenuates cognitive deficits remain unknown and are complex and multifactorial. Our results provide compelling evidence of a correlation among decreased oxidative insult, microglial activation, and behavioral outcome. Specifically, our results demonstrate that 3-NT and Iba1 immunoreactivity in the ipsilateral hippocampus inversely correlated with beam-balance and beam-walk scores, but directly correlated with spatial learning parameters. Furthermore, we found a robust increase in the content of NMDAR1. Excessive or prolonged exposure to glutamate causes NMDAR activation, which increases Ca^{2+} entry into the post-synaptic cell and stimulates the production of nitric oxide by neuronal nitric oxide synthase. Nitric oxide contributes to 3-NT formation and activates downstream signaling pathways, resulting in mitochondrial dysfunction. It should be noted that a limitation of our analysis is that we correlated outcomes that occur days to weeks apart from each other. The correlations were conducted after all the behaviors were concluded, which is two weeks from the motor tasks, while spatial learning was completed 24 h prior to sacrifice.

Several studies have examined the role of NMDAR2, which plays a central role in synaptic plasticity, learning and memory, on TBI. NMDAR2 was significantly decreased in the rat hippocampus, thereby resulting in diminished plasma membrane stability following TBI (Sharma et al., 2010). Rats treated with glutathione showed downregulated NR2B gene expression and had a protective effect against the long-term sequelae of TBI (Arifin et al., 2011). Following TBI, NR2B signaling promoted the amount of autophagic proteins (such as Beclin-1) in membrane rafts of the rat cerebral cortex (Bigford et al., 2009).

Nevertheless, further research is needed to study the potential effects of NMDAR1 on TBI. RNAi-mediated downregulation of aquaporin 4 led to reduced mRNA expression levels and protein content of NMDAR1 in TBI rats (Chen et al., 2018). In our study, TBI rats showed elevated NMDAR1 immunoreactive signal but exposure to EE resulted in a significant decrease in NMDAR1 levels, suggestive of declined glutamate toxicity and ion influx, which inactivates cell death signaling cascades through inhibition of several degradative enzymes, including proteases and endonucleases. Therefore, modulation of NMDAR may be an effective therapeutic target for TBI. Indeed, NMDAR antagonists such as gacyclidine and memantine improve functional and neurological outcome in animal models of TBI (Smith et al., 2000; Rao et al., 2001) but all clinical trials using NMDAR antagonists have failed to show efficacy following TBI and, in some cases, have even increased mortality. A major problem includes a limited neuroprotective therapeutic time window as NMDAR antagonists appear to be highly efficacious when administered prior or immediately (< 30 min) post-injury (Rod and Auer, 1989; Kroppenstedt et al., 1998). In addition, NMDAR antagonists can alter synaptic function and plasticity and induce neurotoxicity (Ikonomidou and Turski, 2002).

In summary, we hypothesize that after moderate-to-severe CCI in adult rats, there is an upstream activation of NMDAR and concomitant oxidative damage and neuroinflammatory process, thereby leading to impaired behavioral functioning. Exposure to EE decreases the concentration of NMDAR and concomitant 3-NT, 4-HNE, and Iba1 immunoreactivity in the rat brain, which was associated with improved spatial learning and memory. Our findings support the notion that an enriched and interactive environment could be of therapeutic interest and benefit for patients with TBI.

Declaration of Competing Interest

None.

Data availability

Data will be made available on request.

Acknowledgements

This work was supported, in part, by the National Institutes of Health grant NS084967 (AEK), the Research Advisory Committee, Children's Hospital of Pittsburgh of UPMC (COB), the María Zambrano Excellence Program from the Ministry of Science and Innovation and the

University of Valladolid, Spain (VT), and the Internationalization program of Junta de Castilla y Leon, Spain (CL-EI-2021-09 IBGM, VT).

References

Arifin, M.Z., Faried, A., Shahib, M.N., Wiriadisastra, K., Bisri, T., 2011. Inhibition of activated NR2B gene- and caspase-3 protein-expression by glutathione following traumatic brain injury in a rat model. Asian J. Neurosurg. 6, 72–77.

Bao, G.C., Bleimeister, I.H., Zimmerman, L.A., Wellcome, J.L., Niesman, P.J., Radabaugh, H.L., Bondi, C.O., Kline, A.E., 2019. Intermittent administration of haloperidol after cortical impact injury neither impedes spontaneous recovery nor attenuates the efficacy of environmental enrichment. J. Neurotrauma 36, 1606–1614.

Beal, M.F., Chiluwal, J., Calingasan, N.Y., Milne, G.L., Shchepinov, M.S., Tapias, V., 2020. Isotope-reinforced polyunsaturated fatty acids improve Parkinson's disease-like phenotype in rats overexpressing alpha-synuclein. Acta Neuropathol. Commun. 8, 220.

Bigford, G.E., Alonso, O.F., Dietrich, D., Keane, R.W., 2009. A novel protein complex in membrane rafts linking the NR2B glutamate receptor and autophagy is disrupted following traumatic brain injury. J. Neurotrauma 26, 703–720.

Block, M.L., Zecca, L., Hong, J.S., 2007. Microglia-mediated neurotoxicity: uncovering the molecular mechanisms. Nat. Rev. Neurosci. 8, 57–69.

Bondi, C.O., Klitsch, K.C., Leary, J.B., Kline, A.E., 2014. Environmental enrichment as a viable neurorehabilitation strategy for experimental traumatic brain injury. J. Neurotrauma 31, 873–888.

Chandra, A., Srivastava, S.K., 1997. A synthesis of 4-hydroxy-2-trans-nonenal and 4-(3H) 4-hydroxy-2-trans-nonenal. Lipids 32, 779–782.

Chen, L.H., Zhang, H.T., Xu, R.X., Li, W.D., Zhao, H., Yang, Y., Sun, K., 2018. Interaction of aquaporin 4 and N-methyl-D-aspartate NMDA receptor 1 in traumatic brain injury of rats. Iran J. Basic Med. Sci. 21, 1148–1154.

Coughlin, J.M., Wang, Y., Minn, I., Bienko, N., Ambinder, E.B., Xu, X., Peters, M.E., Dougherty, J.W., Vranesic, M., Koo, S.M., Ahn, H.H., Lee, M., Cottrell, C., Sair, H.I., Sawa, A., Munro, C.A., Nowinski, C.J., Dannals, R.F., Lyketsos, C.G., Kassiou, M., Smith, G., Caffo, B., Mori, S., Guilarte, T.R., Pomper, M.G., 2017. Imaging of glial cell activation and white matter integrity in brains of active and recently retired national football league players. JAMA Neurol. 74, 67–74.

Crane, P.K., Gibbons, L.E., Dams-O'Connor, K., Trittschuh, E., Leverenz, J.B., Keene, C.D., Sonnen, J., Montine, T.J., Bennett, D.A., Leurgans, S., Schneider, J.A., Larson, E.B., 2016. Association of traumatic brain injury with late-life neurodegenerative conditions and neuropathologic findings. JAMA Neurol. 73, 1062–1069.

Darwish, R.S., Amiridze, N., Aarabi, B., 2007. Nitrotyrosine as an oxidative stress marker: evidence for involvement in neurologic outcome in human traumatic brain injury. J. Trauma 63, 439–442.

de la Tremblaye, P.B., Cheng, J.P., Bondi, C.O., Kline, A.E., 2019. Environmental enrichment, alone or in combination with various pharmacotherapies, confers marked benefits after traumatic brain injury. Neuropharmacology 145, 13–24.

de la Tremblaye, P.B., Wellcome, J.L., Wiley, K., Lomahan, C.A., Moschonas, E.H., Cheng, J.P., Bondi, C.O., Kline, A.E., 2021. Chronic unpredictable stress during adolescence protects against adult traumatic brain injury-induced affective and cognitive deficits. Brain Res. 1767, 147544.

de Witt, B.W., Ehrenberg, K.M., McAloon, R.L., Panos, A.H., Shaw, K.E., Raghavan, P.V., Skidmore, E.R., Kline, A.E., 2011. Abbreviated environmental enrichment enhances neurobehavioral recovery comparably to continuous exposure after traumatic brain injury. Neurorehabil. Neural Repair 25, 343–350.

Deng, Y., Thompson, B.M., Gao, X., Hall, E.D., 2007. Temporal relationship of peroxynitrite-induced oxidative damage, calpain-mediated cytoskeletal degradation and neurodegeneration after traumatic brain injury. Exp. Neurol. 205, 154–165.

Di Pietro, V., Lazzarino, G., Amorini, A.M., Tavazzi, B., D'Urso, S., Longo, S., Vagnozzi, R., Signoretti, S., Clementi, E., Giardina, B., Lazzarino, G., Belli, A., 2014. Neuroglobin expression and oxidant/antioxidant balance after graded traumatic brain injury in the rat. Free Radic. Biol. Med. 69, 258–264.

Diaz-Chavez, A., Lajud, N., Roque, A., Cheng, J.P., Melendez-Herrera, E., Valdez-Alarcon, J.J., Bondi, C.O., Kline, A.E., 2020. Early life stress increases vulnerability to the sequelae of pediatric mild traumatic brain injury. Exp. Neurol. 329, 113318.

Frick, K.M., Fernandez, S.M., 2003. Enrichment enhances spatial memory and increases synaptophysin levels in aged female mice. Neurobiol. Aging 24, 615–626.

Gardner, R.C., Byers, A.L., Barnes, D.E., Li, Y., Boscardin, J., Yaffe, K., 2018. Mild TBI and risk of Parkinson disease: a chronic effects of Neurotrauma consortium study. Neurology 90, e1771–e1779.

Hall, E.D., Vaishnav, R.A., Mustafa, A.G., 2010. Antioxidant therapies for traumatic brain injury. Neurotherapeutics 7, 51–61.

Higashi, Y., Hoshijima, M., Yawata, T., Nobumoto, A., Tsuda, M., Shimizu, T., Saito, M., Ueba, T., 2014. Suppression of oxidative stress and 5-lipoxygenase activation by edaravone improves depressive-like behavior after concussion. J. Neurotrauma 31, 1689–1699.

Hill, R.L., Singh, I.N., Wang, J.A., Hall, E.D., 2017. Time courses of post-injury mitochondrial oxidative damage and respiratory dysfunction and neuronal cytoskeletal degradation in a rat model of focal traumatic brain injury. Neurochem. Int. 111, 45–56.

Hyder, A.A., Wunderlich, C.A., Puvanachandra, P., Gururaj, G., Kobusingye, O.C., 2007. The impact of traumatic brain injuries: a global perspective. NeuroRehabilitation 22, 341–353.

Ikonomidou, C., Turski, L., 2002. Why did NMDA receptor antagonists fail clinical trials for stroke and traumatic brain injury? Lancet Neurol. 1, 383–386.

Itoh, T., Satou, T., Nishida, S., Tsubaki, M., Hashimoto, S., Ito, H., 2009. The novel free radical scavenger, edaravone, increases neural stem cell number around the area of damage following rat traumatic brain injury. Neurotox. Res. 16, 378–389.

Ji, X., Liu, W., Xie, K., Liu, W., Qu, Y., Chao, X., Chen, T., Zhou, J., Fei, Z., 2010. Beneficial effects of hydrogen gas in a rat model of traumatic brain injury via reducing oxidative stress. Brain Res. 1354, 196–205.

Johnson, E.M., Traver, K.L., Hoffman, S.W., Harrison, C.R., Herman, J.P., 2013. Environmental enrichment protects against functional deficits caused by traumatic brain injury. Front. Behav. Neurosci. 7, 44.

Jove, M., Mota-Martorell, N., Pradas, I., Martin-Gari, M., Ayala, V., Pamplona, R., 2020. The advanced lipoxidation end-product malondialdehyde-lysine in aging and longevity. Antioxidants (Basel) 9.

Kline, A.E., Massucci, J.L., Marion, D.W., Dixon, C.E., 2002. Attenuation of working memory and spatial acquisition deficits after a delayed and chronic bromocriptine treatment regimen in rats subjected to traumatic brain injury by controlled cortical impact. J. Neurotrauma 19, 415–425.

Kline, A.E., McAloon, R.L., Henderson, K.A., Bansal, U.K., Ganti, B.M., Ahmed, R.H., Gibbs, R.B., Sozda, C.N., 2010. Evaluation of a combined therapeutic regimen of 8-OH-DPAT and environmental enrichment after experimental traumatic brain injury. J. Neurotrauma 27, 2021–2032.

Kline, A.E., Leary, J.B., Radabaugh, H.L., Cheng, J.P., Bondi, C.O., 2016. Combination therapies for neurobehavioral and cognitive recovery after experimental traumatic brain injury: is more better? Prog. Neurobiol. 142, 45–67.

Knopp, R.C., Lee, S.H., Hollas, M., Nepomuceno, E., Gonzalez, D., Tam, K., Aamir, D., Wang, Y., Pierce, E., BenAissa, M., Thatcher, G.R.J., 2020. Interaction of oxidative stress and neurotrauma in ALDH2(−/−) mice causes significant and persistent behavioral and pro-inflammatory effects in a tractable model of mild traumatic brain injury. Redox Biol. 32, 101486.

Kokiko, O.N., Hamm, R.J., 2007. A review of pharmacological treatments used in experimental models of traumatic brain injury. Brain Inj. 21, 259–274.

Kroppenstedt, S.N., Schneider, G.H., Thomale, U.W., Unterberg, A.W., 1998. Protective effects of aptiganel HCl (Cerestat) following controlled cortical impact injury in the rat. J. Neurotrauma 15, 191–197.

Lajud, N., Diaz-Chavez, A., Radabaugh, H.L., Cheng, J.P., Rojo-Soto, G., Valdez-Alarcon, J.J., Bondi, C.O., Kline, A.E., 2019. Delayed and abbreviated environmental enrichment after brain trauma promotes motor and cognitive recovery that is not contingent on increased neurogenesis. J. Neurotrauma 36, 756–767.

Loane, D.J., Kumar, A., Stoica, B.A., Cabatbat, R., Faden, A.I., 2014. Progressive neurodegeneration after experimental brain trauma: association with chronic microglial activation. J. Neuropathol. Exp. Neurol. 73, 14–29.

LoBue, C., Wilmoth, K., Cullum, C.M., Rossetti, H.C., Lacritz, L.H., Hynan, L.S., Hart, Jr, J., Womack, K.B., 2016. Traumatic brain injury history is associated with earlier age of onset of frontotemporal dementia. J. Neurol. Neurosurg. Psychiatry 87, 817–820.

Maegele, M., Lippert-Gruener, M., Ester-Bode, T., Sauerland, S., Schafer, U., Molcanyi, M., Lefering, R., Bouillon, B., Neiss, W.F., Angelov, D.N., Klug, N., McIntosh, T.K., Neugebauer, E.A., 2005. Reversal of neuromotor and cognitive dysfunction in an enriched environment combined with multimodal early onset stimulation after traumatic brain injury in rats. J. Neurotrauma 22, 772–782.

Mallah, K., Couch, C., Borucki, D.M., Toutonji, A., Alshareef, M., Tomlinson, S., 2020. Anti-inflammatory and neuroprotective agents in clinical trials for CNS disease and injury: where do we go from here? Front. Immunol. 11, 2021.

Margulies, S., Anderson, G., Atif, F., Badaut, J., Clark, R., Empey, P., Guseva, M., Hoane, M., Huh, J., Pauly, J., Raghupathi, R., Scheff, S., Stein, D., Tang, H., Hicks, M., 2016. Combination therapies for traumatic brain injury: retrospective considerations. J. Neurotrauma 33, 101–112.

McKee, A.C., Stern, R.A., Nowinski, C.J., Stein, T.D., Alvarez, V.E., Daneshvar, D.H., Lee, H.S., Wojtowicz, S.M., Hall, G., Baugh, C.M., Riley, D.O., Kubilus, C.A., Cormier, K.A., Jacobs, M.A., Martin, B.R., Abraham, C.R., Ikezu, T., Reichard, R.R., Wolozin, B.L., Budson, A.E., Goldstein, L.E., Kowall, N.W., Cantu, R.C., 2013. The spectrum of disease in chronic traumatic encephalopathy. Brain 136, 43–64.

Miyamoto, K., Ohtaki, H., Dohi, K., Tsumuraya, T., Song, D., Kiriyama, K., Satoh, K., Shimizu, A., Aruga, T., Shioda, S., 2013. Therapeutic time window for edaravone treatment of traumatic brain injury in mice. Biomed. Res. Int. 2013, 379206.

Moretti, L., Cristofori, I., Weaver, S.M., Chau, A., Portelli, J.N., Grafman, J., 2012. Cognitive decline in older adults with a history of traumatic brain injury. Lancet Neurol. 11, 1103–1112.

Morgan, M.J., Liu, Z.G., 2011. Crosstalk of reactive oxygen species and NF-kappaB signaling. Cell Res. 21, 103–115.

Moschonas, E.H., Leary, J.B., Memarzadeh, K., Bou-Abboud, C.E., Folweiler, K.A., Monaco, C.M., Cheng, J.P., Kline, A.E., Bondi, C.O., 2021. Disruption of basal forebrain cholinergic neurons after traumatic brain injury does not compromise environmental enrichment-mediated cognitive benefits. Brain Res. 1751, 147175.

Passineau, M.J., Green, E.J., Dietrich, W.D., 2001. Therapeutic effects of environmental enrichment on cognitive function and tissue integrity following severe traumatic brain injury in rats. Exp. Neurol. 168, 373–384.

Picklo, M.J., Montine, T.J., 2001. Acrolein inhibits respiration in isolated brain mitochondria. Biochim. Biophys. Acta 1535, 145–152.

Radabaugh, H.L., Carlson, L.J., O'Neil, D.A., LaPorte, M.J., Monaco, C.M., Cheng, J.P., de la Tremblaye, P.B., Lajud, N., Bondi, C.O., Kline, A.E., 2016. Abbreviated environmental enrichment confers neurobehavioral, cognitive, and histological benefits in brain-injured female rats. Exp. Neurol. 286, 61–68.

Ramlackhansingh, A.F., Brooks, D.J., Greenwood, R.J., Bose, S.K., Turkheimer, F.E., Kinnunen, K.M., Gentleman, S., Heckemann, R.A., Gunanayagam, K., Gelosa, G., Sharp, D.J., 2011. Inflammation after trauma: microglial activation and traumatic brain injury. Ann. Neurol. 70, 374–383.

Rao, V.L., Dogan, A., Todd, K.G., Bowen, K.K., Dempsey, R.J., 2001. Neuroprotection by memantine, a non-competitive NMDA receptor antagonist after traumatic brain

injury in rats. Brain Res. 911, 96–100.
Readnower, R.D., Chavko, M., Adeeb, S., Conroy, M.D., Pauly, J.R., McCarron, R.M., Sullivan, P.G., 2010. Increase in blood-brain barrier permeability, oxidative stress, and activated microglia in a rat model of blast-induced traumatic brain injury. J. Neurosci. Res. 88, 3530–3539.
Rod, M.R., Auer, R.N., 1989. Pre- and post-ischemic administration of dizocilpine (MK-801) reduces cerebral necrosis in the rat. Can. J. Neurol. Sci. 16, 340–344.
Sharma, S., Ying, Z., Gomez-Pinilla, F., 2010. A pyrazole curcumin derivative restores membrane homeostasis disrupted after brain trauma. Exp. Neurol. 226, 191–199.
Smith, J.S., Fulop, Z.L., Levinsohn, S.A., Darrell, R.S., Stein, D.G., 2000. Effects of the novel NMDA receptor antagonist gacyclidine on recovery from medial frontal cortex contusion injury in rats. Neural. Plast. 7, 73–91.
Solaroglu, I., Okutan, O., Kaptanoglu, E., Beskonakli, E., Kilinc, K., 2005. Increased xanthine oxidase activity after traumatic brain injury in rats. J. Clin. Neurosci. 12, 273–275.
Sozda, C.N., Hoffman, A.N., Olsen, A.S., Cheng, J.P., Zafonte, R.D., Kline, A.E., 2010. Empirical comparison of typical and atypical environmental enrichment paradigms on functional and histological outcome after experimental traumatic brain injury. J. Neurotrauma 27, 1047–1057.
Sullivan, P.G., Keller, J.N., Mattson, M.P., Scheff, S.W., 1998. Traumatic brain injury alters synaptic homeostasis: implications for impaired mitochondrial and transport function. J. Neurotrauma 15, 789–798.
Sun, Y., Bai, L., Niu, X., Wang, Z., Yin, B., Bai, G., Zhang, D., Gan, S., Sun, C., Wang, S., Zhu, F., Zhang, M., 2019. Elevated serum levels of inflammation-related cytokines in mild traumatic brain injury are associated with cognitive performance. Front. Neurol. 10, 1120.
van Praag, H., Kempermann, G., Gage, F.H., 2000. Neural consequences of environmental enrichment. Nat. Rev. Neurosci. 1, 191–198.
Wolf, J.A., Koch, P.F., 2016. Disruption of network synchrony and cognitive dysfunction after traumatic brain injury. Front. Syst. Neurosci. 10, 43.
Yu, K.W., Wang, C.J., Wu, Y., Wang, Y.Y., Wang, N.H., Kuang, S.Y., Liu, G., Xie, H.Y., Jiang, C.Y., Wu, J.F., 2020. An enriched environment increases the expression of fibronectin type III domain-containing protein 5 and brain-derived neurotrophic factor in the cerebral cortex of the ischemic mouse brain. Neural Regen. Res. 15, 1671–1677.